JOURNAL OF GEOPHYSICAL RESEARCH, VOL. 91, NO. C2, PAGES 2607–2615, FEBRUARY 15, 1986

Persistence of a Pattern of Surface Gravity Waves

KENNETH M. WATSON

Marine Physical Laboratory of the Scripps Institution of Oceanography, University of California, San Diego

The observation of ship Kelvin wakes by the Seasat synthetic aperture radar raises a question concerning the persistence of patterns of surface gravity waves. Time scales vary with wavelength and environmental conditions. The range extends from fractions of a second at the shortest wavelengths to many days for ocean swell. Several mechanisms for destroying a wave pattern are investigated here. These are viscous dissipation, direct wind-wave interaction, and nonlinear hydrodynamic interaction with ambient surface waves. The nonlinear hydrodynamic interactions appear to be the most significant.

1. Introduction

The imaging of surface ship Kelvin wakes by the Seasat synthetic aperture radar (SAR) raises an interesting question: How long will a given "pattern" of surface waves persist? Under conditions of light wind and low sea state the Kelvin wake of a vessel may be seen to persist astern for some kilometers. Under more robust sea conditions the wake persistence seems to be greatly reduced. In this paper we shall discuss several mechanisms contributing to the decay of such a "pattern."

Deterministic mechanisms, such as linear wave propagation and dispersion and the interaction with known large-scale currents, can distort a wave pattern. This, however, is in principle predictable and will not be considered as "pattern decay." Stochastic mechanisms, such as interaction with wind and ambient sea, do lead to a genuine decay of the pattern. We note, however, that the quantitative criteria for decay may be sensitive to the detection algorithm used.

We shall be principally concerned here with the decay of gravity waves in the 0.1- to 4-m range of wavelengths. The mechanisms considered for decay imply a strong sensitivity to wavelength. For wavelengths less than 10 cm the time scales as predicted are too short (of the order of a second, or less) to be of interest in the present context. For wavelengths greater than a few meters the predicted time scales become so long that changing environmental conditions may be a factor. Patterns of swell have been observed to propagate across ocean basins [*Snodgrass et al.*, 1966]. The Bragg wavelengths for the Seasat SAR were in the 30-cm range [*Vesecky and Stewart*, 1982], which is well within the scope of our analysis.

There are evidently several mechanisms that contribute to wave pattern decay. Viscous dissipation seems to be the simplest of these. Wind-wave interaction, while physically complex, is phenomenologically modeled as a simple exponential pattern decay. These mechanisms are reviewed in section 3.

Nonlinear hydrodynamic interactions of the pattern with ambient surface waves provide other decay mechanisms. In the terminology of wave-wave weak interaction theory, both "three-wave" and "four-wave" interactions must be considered. It is well-known that for gravity waves the three-wave interactions do not admit resonant frequency conditions. We shall see that these lead to only partial pattern decay. Only if this decay brings the signal-to-noise level below the threshold for detectability, can we consider the pattern destroyed. The four-wave interactions act on a slower time scale than do the three-wave interactions, but lead to total decay of the pattern (according to weak interaction theories).

In section 4 we discuss first the three- and four-wave interactions of pattern waves with ambient waves of much longer wavelengths. The response to a matched filter in the space time domain will be described using a technique due to *Van Kampen* [1974].

In section 4 we also analyze the pattern response to interaction with waves of similar wavelengths. A formulation of the *Hasselmann* [1967] equations given by *Dungey and Hui* [1979] is used for this.

The evolution of the pattern spectrum is investigated in section 5. For the case of three-wave interactions this is done explicitly. The effect of four-wave interactions with long waves is formulated in terms of diffusion equation in wave number space.

The conclusions of this paper are summarized in section 6. It is observed that the fastest decay rates obtained result from three-wave interaction with long ambient waves. When this mechanism is not effective, the dominant decay mechanism is four-wave resonant interactions with long ambient waves, with the wind mechanism being somewhat comparable.

2. Description of the Decay Phenomena

In a specified "rectangular area of ocean" we use a Fourier expansion for the surface wave displacement $\zeta(\boldsymbol{x}, t)$ ($\boldsymbol{x} = x, y$, *a* vector in the plane of the quiescent ocean surface):

$$\zeta(\boldsymbol{x}, t) = -Im\ [Z(\boldsymbol{x}, t)]$$
$$Z(\boldsymbol{x}, t) = \sum_l b_l \exp\left[i\boldsymbol{l}\cdot\boldsymbol{x} - \omega_l t\right] \qquad (1)$$

Here $\omega_l = (gl)^{1/2}$. In the approximation that the waves are

Paper number 5C0699.
0148-0227/86/005C-0699$05.00

linear and not forced, the b_l are constants. In general, $b_l(t)$ is time dependent.

We shall suppose that (1) refers to the ambient sea. For the pattern waves we take as a special case of (1),

$$\zeta_p(\boldsymbol{x}, t) = -Im\ (Z_p)$$
$$Z_P = \sum_k B_k(t) \exp [i(\boldsymbol{k} \cdot \boldsymbol{x} - \omega_k t)] \qquad (2)$$

We shall suppose that the $B_k(0)$ are fixed, specified amplitudes (they determine the pattern) at some reference time, say, t = 0.

Over an ensemble of realizations of the ocean surface the b_l will be considered to be uncorrelated Gaussian variables. The ensemble averaged spectrum Ψ_a of vertical displacement is

$$\Psi_a(l)\, d^2l = \sum_l \tfrac{1}{2} < |b_l|^2 > \qquad (3)$$

In this paper we shall use a *Pierson and Moskowitz* [1964] spectrum for the ambient sea:

$$\Psi(l) = \left(\frac{\eta}{l^4}\right) \exp [-0.74 \left(\frac{l_o}{l}\right)^2] G(\theta)$$
$$\eta = 4 \cdot 10^{-3}, \qquad l_o = g/W^2 \qquad (4)$$

Here $\boldsymbol{W}$ is the wind velocity, g = 9.8 m/s^2, and θ is the angle between $\boldsymbol{l}$ and $\boldsymbol{W}$. We shall specify models of $G(\theta)$ later, but now note the normalization

$$\int_{-\pi}^{\pi} G(\theta)\, d\theta = 1 \qquad (5)$$

For the pattern waves, we introduce the *Wigner* [1932] correlation function

$$\Gamma_p(\boldsymbol{r}, \boldsymbol{x}, t) = \tfrac{1}{2} < Z_p(\boldsymbol{x} - \boldsymbol{r}/2, t) Z_p^*(\boldsymbol{x} + \boldsymbol{r}/2, t) > \qquad (6)$$

Here < > represents an ensemble average over the ambient sea, as in (3). In performing this ensemble average the pattern amplitudes $B_k(0)$ are considered deterministic and fixed. The spectrum of vertical displacement is

$$\Psi_p(\boldsymbol{k}, \boldsymbol{x}, t) = \int \Gamma_p \exp (i\boldsymbol{k} \cdot \boldsymbol{r})\, d^2r/(2\pi)^2 \qquad (7)$$

(It is assumed that $\boldsymbol{x}$ varies slowly over distances comparable to pattern wavelengths of interest.)

The spectrum of wave action F and energy E are related to the spectrum of vertical displacement Ψ by the relations

$$F = (g\rho_o/\omega_k)\Psi = E/\omega_k \qquad (8)$$

where ρ_o is the density of seawater. The *Hasselmann* [1967] equation for the evolution of F is of the form

$$\frac{\partial F}{\partial t} + \dot{\boldsymbol{x}} \cdot \nabla_x F = S_{nl} + S_v + S_w \qquad (9)$$

Here $\dot{\boldsymbol{x}} = \nabla_k \omega_k$, and S_{nl}, S_v, and S_w represent the effects of wave-wave interactions, viscosity, and wind, respectively. We have omitted the term in (9) describing diffraction by large-scale surface currents or shoaling. To the extent that such effects are known, their influence on the pattern is predictable and would not lead to pattern decay. These effects are sensitive to detail and seem best omitted in the present general discussion.

We may write

$$F = F_a + F_p \qquad (10)$$

where F_a refers to the action spectrum of ambient waves and F_p to that of the pattern waves. For simplicity, we take F_a to be a (quasi) stationary solution to (9). Then, on inserting (10) into (9) and linearizing in F_p, we obtain

$$\frac{\partial F_p}{\partial t} + \dot{\boldsymbol{x}} \cdot \nabla_x F_p = S_n' + S_v' + S_w' \qquad (11)$$

The quantities on the right depend linearly on F_p and will be specified later.

3. Effects of Viscosity and Wind

Viscosity will lead to exponential damping of the pattern waves. In the notation of (11) this is expressed as [*Phillips*, 1977]

$$S_v' = -\beta_v F_p$$
$$\beta_v = 4\nu_o k^2 \qquad (12)$$

where $\nu_o \cong 1.1 \cdot 10^{-6}\ m^2/s$ is the kinematic viscosity of seawater. The decay time

$$T_d(v) \equiv \beta_v^{-1} \qquad (13)$$

is shown as a function of wavelength $\lambda = 2\pi/k$ in Figure 1.

The rate of wind-induced growth for surface waves has recently been reviewed by *Plant* [1982; see also, *Mitsuyasu and Honda*, 1982]. He concludes that for the growth rate of small amplitude waves,

$$S_w' = \beta_w F_p \qquad (14)$$

in (9). Here

$$\beta_w = 0.04 u_*^2 k^2 \cos\theta/\omega_k \qquad (15)$$

where u_* is the friction velocity of the wind and θ is the angle between $\boldsymbol{k}$ and $\boldsymbol{W}$.

It seems plausible for our purposes to interpret

$$T_d(w) \equiv \beta_w^{-1} \qquad (16)$$

as a pattern decay time.

To evaluate (16) we use the analysis of *Garratt* [1977] to relate u_* to the wind speed W at 10-m height. The resulting time $T_d(w)$ is shown in Figure 2 as a function of W for several wavelengths λ and angle $\theta = 0$. We note from Figures 1 and 2 that for $W > 2\ m/s$, $T_d(w) < T_d(v)$ when $\lambda > 0.1$ m.

4. Effects of Wave-Wave Interactions

One simple descriptor of pattern decay is given by the correlation function, which we may consider as the output of a "matched filter."

$$\Gamma_0(t) = < P[\zeta_p(\boldsymbol{x}, 0); t] \zeta_p(\boldsymbol{x}, t) > \qquad (17)$$

Here $t = 0$ is considered to be the reference time at which the pattern is first observed. The quantity

$$P[\zeta_p(\boldsymbol{x}, 0; t)]$$

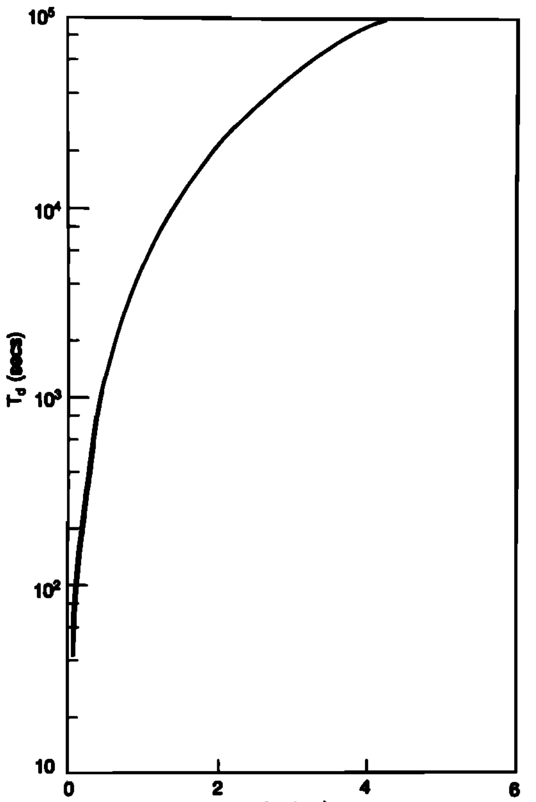

Fig. 1. The decay time (13) due to viscous dissipation as a function of wavelength.

represents the predicted field at t, given the initial field $\zeta_p(x, 0)$. The prediction is to be obtained using known deterministic phenomena that may distort the pattern. For example, if linear wave propagation is the only deterministic phenomenon, then

$$P[\zeta_p(x, 0); t] = -Im \sum_k \left\{ B_k(0) \exp\left[i(k \cdot x - \omega_k t)\right] \right\} \quad (18)$$

where $B_k(0)$ is the value of B_k at $t = 0$.

The ensemble average in (17) is considered to be one over realizations of the ambient field amplitudes b_k (see (1)) with the initial pattern amplitudes $B_k(0)$ being fixed, as in (6). If the pattern could be predicted exactly at time t, then $\Gamma_0(t)$ would represent the mean square pattern vertical displacement. Interaction of the pattern with the ambient wave field reduces the accuracy of this prediction and leads to a mismatch between the predicted and actual patterns, causing the correlation, or "filter output," Γ_0 to decay with time.

In this paper we shall assume that (18) applies to evaluating (17). Then it is sufficient to calculate the set of correlations

$$\gamma_{kk'}(t) = \langle B_k(t) B_{k'}(0) \rangle = \langle B_k(t) \rangle B_{k'}(0) \quad (19)$$

We shall refer to a given Fourier amplitude in the pattern as a "test wave."

Under certain conditions we might expect $\langle B_k \rangle$ to be determined from a Langevin equation of the form

$$\frac{d}{dt} \langle B_k \rangle = -\nu(k) \langle B_k \rangle \quad (20)$$

where $\nu(k)$ is the Langevin "rate constant." In this case we would evaluate (19) as

$$\gamma_{kk'} = B_k(0) B_{k'}(0) \exp\left[-\nu(k) t\right] \quad (21)$$

We shall see that four-wave interactions, with frequency resonance, lead asymptotically to equations of the form (20) and (21).

4.1. Interaction with Ambient Wave Orbital Currents

As a first illustration of (17) and (19) we consider the advection of a test wave k due to the orbital velocity $U(x, t)$ of the ambient waves. This current is of the form

$$U(x, t) = \sum_l \left(\frac{i}{2}\right) \hat{l} \omega_l \left\{ b_l \exp\left[i(l \cdot x - \omega_l t)\right] - c.c \right\} \quad (22)$$

where $\hat{l} \equiv l/l$, using the notation of (1). We may assume here that the ambient waves are linear, so the b_l are constants. We shall also assume that

$$l \ll k \quad (23)$$

or the wavelength of the test wave is small compared with that of those ambient waves which are of most importance for pattern decorrelation. This assumption can be tested for verification when we evaluate the decay using the spectrum (4).

If the test wave is advected with the local velocity U, we use (23) to write

$$B_k(t) \cong B_k(0) \exp\left[-ik \cdot \int_0^t U(t') \, dt'\right] \quad (24)$$

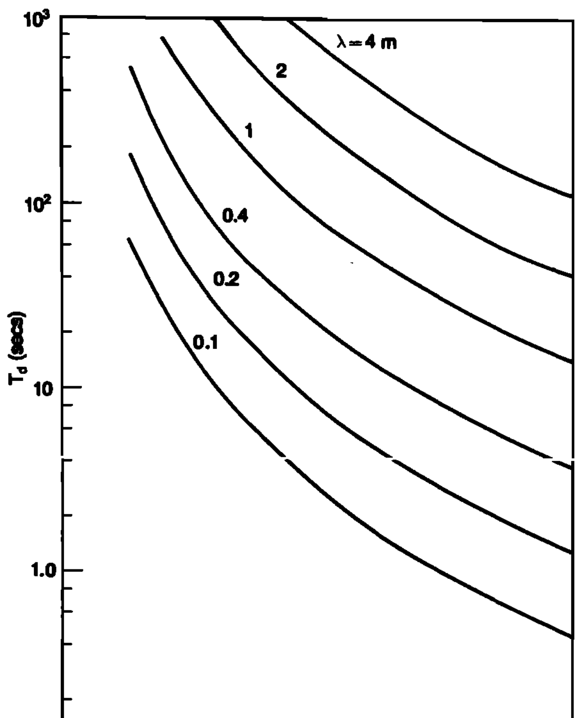

Fig. 2. The decay time (16) due to wind-sea interaction as a function of wind speed for several wavelengths.

Using the assumed Gaussian distribution of the b_k's and the relation (3), we obtain

$$< B_k(t) > = B_k(0) \exp [-D_3(\boldsymbol{k}, t)] \quad (25)$$

where

$$D_3(\boldsymbol{k}, t) = \int d^2l\,(\boldsymbol{k}\cdot\hat{l})^2\,[1 - \cos(\omega_l t)]\Psi_a(\boldsymbol{l}) \quad (26)$$

For small t this becomes

$$D_3(\boldsymbol{k}, t) \cong \sigma^2 t^2/2 \quad , \quad \omega_{l_0}(t) << 1 \quad (27)$$

where

$$\sigma^2 = < (\boldsymbol{k}\cdot\boldsymbol{U})^2 > = \int d^2l\,(\boldsymbol{k}\cdot\hat{l})^2 \omega_l^2 \Psi_a(\boldsymbol{l}) \quad (28)$$

For $t \rightarrow \infty$, on the other hand, we have

$$D_3(\boldsymbol{k}, \infty) = \int d^2l\,(\boldsymbol{k}\cdot\hat{l})^2 \Psi_a(\boldsymbol{l}) \quad (29)$$

We note that for the spectrum (4) the assumed condition (23) appears to be valid for the evaluation of D_3.

When (27) is valid, we may define an e-folding decay time as

$$T_d(3) = 2^{1/2}/\sigma \quad (30)$$

More generally, we may define the decay time with the relation

$$D_3[\boldsymbol{k}, T_d(3)] = 1 \quad (31)$$

This equation may or may not have a solution. When there is no solution, the advection mechanism is ineffective in destroying the pattern. The single e-folding condition (31) is arbitrary, and one may wish to define the decay time to correspond to several e-foldings.

The decay relation (25) is not of the form (21). This is due to the lack of a frequency resonance in the wave interactions.

4.2 Decay Due to Three-Wave Interaction

A more systematic and formal description of the decay of (19) can be obtained using the method of *Van Kampen* [1974]. To develop this, we begin with the formulation of *Watson and West* [1975]. Their equation of motion, when linearized in the pattern amplitudes B_k, is of the form

$$\dot{B}_k = T_2(B, b) + T_3(B, b) + \ldots \quad (32)$$

Here T_2 and T_3 are quadratic and cubic, respectively, in wave amplitudes. If we ignore all but the T_2 term, (32) takes the form

$$\dot{B}_k = \sum_p A_k{}^p B_p \quad (33)$$

where

$$A_k^p = \sum_l \delta_{k-l-p} \left\{ 2\Gamma_{pl}^{k} b_l \exp[(\omega_k - \omega_p - \omega_l)t] \right. \\ \left. + \Gamma_p^{k-l} b_{-l}^{*} \exp[i(\omega_k - \omega_p - \omega_l)t] \right\} \quad (34)$$

The coefficients Γ are defined in Appendix A of *Watson and West* [1975].

The Van Kempen equation is

$$\frac{d}{dt} < B_k > = -K(t) < B_k > \quad (35)$$

where

$$K(t) = -\int_0^t d\tau < A_k{}^p(t) A_p{}^k(t-\tau) > \quad (36)$$

Evaluation of this is straightforward, assuming that the b_l are constant and Gaussian and that $l << k, p$. The result is

$$K(t) = \int d^2l\,(\boldsymbol{k}\cdot\hat{l})^2 \omega_l \sin(\omega_l t)\Psi_a(\boldsymbol{l}) \quad (37)$$

Integration of (35) leads to the expression (25) with D_3 given by (26).

The three-wave interaction model (33) is thus equivalent to the simple advection model described by (24). The fact that our decay function D_3 does not increase indefinitely with time reflects the lack of a three-wave resonance. To find true decay to a vanishing pattern amplitude, we include the effects of T_3 in (32). This contains four-wave interactions. Higher order terms arising from T_2 also contribute four-wave interactions and must also be included.

4.3. Decay Due to Four-Wave Interactions

Taking account of the four-wave interactions with long wavelength ambient waves, we again have an equation of the form (33), but with the definition

$$A_k^p = \frac{i}{2} \sum_{l,n} \delta_{k+n-l-p} C_{pl}^{kn} b_l b_n^{*} \\ \cdot \exp[i(\omega_k - \omega_p + \omega_n - \omega_l)t] \quad (38)$$

The coefficients C here are defined in Appendix B of *Watson and West* [1975] (see specifically their equation (47)). Some rapidly oscillating terms have been dropped from (38), since these do not contain frequency resonance and so do not lead to a true pattern decay. It is assumed in (38) that $l, n << k, p$.

Evaluation of (36) using (38) now gives the decay rate

$$\nu(t) = \mathrm{Re}\,[K(t)] \\ \cong \frac{49}{128} \int d^2l\, d^2n\, \Psi_a(\boldsymbol{l})\Psi_a(\boldsymbol{n}) \Big[\boldsymbol{k}\cdot(\omega_n \boldsymbol{l} + \omega_l \boldsymbol{n})\Big]^2 \\ \cdot \frac{\sin(\beta t)}{\beta} \quad (39)$$

where

$$\beta = \omega_l - \omega_n + \omega_k - \omega_{|k+l-n|} \\ \cong \omega_l - \omega_n + \boldsymbol{c}(\boldsymbol{k})\cdot(\boldsymbol{n} - \boldsymbol{l}) \quad (40)$$

and $\boldsymbol{c}(\boldsymbol{k}) = \nabla_k \omega_k$. As $t \rightarrow \infty$, we obtain

$$\nu(\infty) = \frac{49\pi}{128} \int d^2l\, d^2n\, \Psi_a(\boldsymbol{l})\Psi_a(\boldsymbol{n}) \\ \Big[\boldsymbol{k}\cdot(\omega_n \boldsymbol{l} + \omega_l \boldsymbol{n})\Big]^2 \delta(\beta) \quad (41)$$

We see that asymptotically the four-wave resonance leads to a Langevin decay law of the form (21).

For finite times, we have the relation

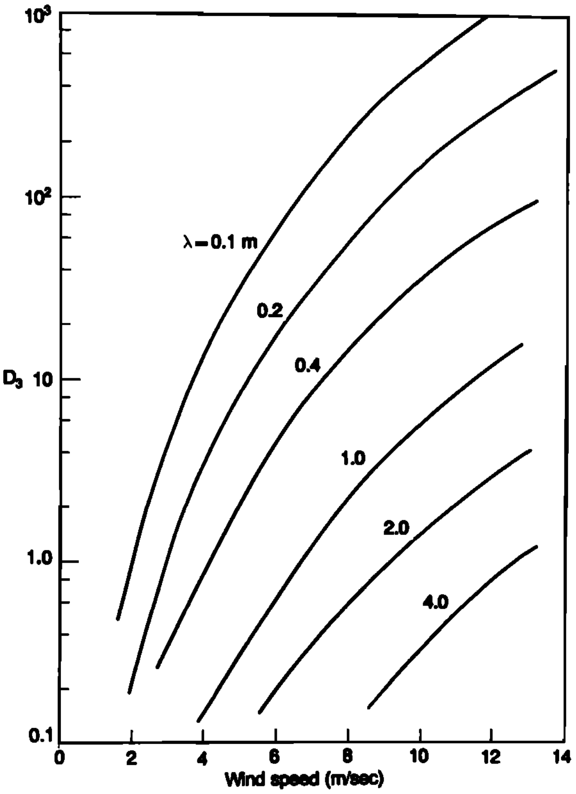

Fig. 3. The limiting decay function (29) due to three-wave interactions as a function of wind speed for several wavelengths.

$$< B_k(t) > = B_k(0) \exp[-D_4(k, t)] \quad (42)$$

where

$$D_4(k, t) = \int_0^t \nu(t')\, dt'$$

$$= \frac{49}{128} \int d^2l\, d^2n\, \Psi_a(l)\Psi_a(n)[k\cdot(l\omega_n + n\omega_l)]^2$$

$$\cdot [1 - \cos(\beta t)]/\beta^2 \quad (43)$$

As $t \rightarrow \infty$, we obtain

$$D_4(k, t) = \nu(\infty)t \quad (44)$$

To describe the implication of (26) and (43), we first assume an isotropic ambient spectrum

$$G(\theta) = 1/(2\pi) \quad (45)$$

Although not realistic as a wind wave spectrum, (45) leads to reasonably accurate decay rates because of the integration over wave angles. A more realistic spectrum will be considered later.

Using (45), we can readily express (26) in the form

$$D_3(k, t) = (\frac{\eta}{2})(k/l_o)^2 J_3(s)$$

$$J_3(s) = \int_1^\infty [1 - \cos(x^{1/2}s)\, dx/x^3 \quad (46)$$

where

$$s \equiv \omega_{l_0} t \quad (47)$$

and we have replaced the exponential factor in (4) by a simple cutoff at $l = l_0$. Similarly, we may evaluate (43) as

$$D_4(k, t) = (\frac{49}{96}\eta^2(k/l_o)^2 s J_4(s)$$

$$J_4(s) = \frac{\pi}{2} + s^3 \int_0^\infty \frac{[1 - \cos u]du}{(u+s)^3 u^2} \quad (48)$$

In Figure 3 we show the limiting decay (29) for three-wave interactions for several wavelengths $\lambda = 2\pi/k$ as functions of wind speed W. When $D_3(k, \infty)$ is small enough that the pattern cannot be considered destroyed, the three-wave mechanism is ineffective. We have arbitrarily chosen here

$$D_3(k, \infty) \geqslant 1 \quad (49)$$

as the condition of pattern destruction by three-wave interactions.

We now define a decay time T_d as being the smaller of T_3, T_4 where

$$D_3(k, T_3) = 1$$
$$D_4(k, T_4) = 1 \quad (50)$$

In Figure 4 we show T_d as a function of wind speed for several wavelengths λ. The dashed lines represent an

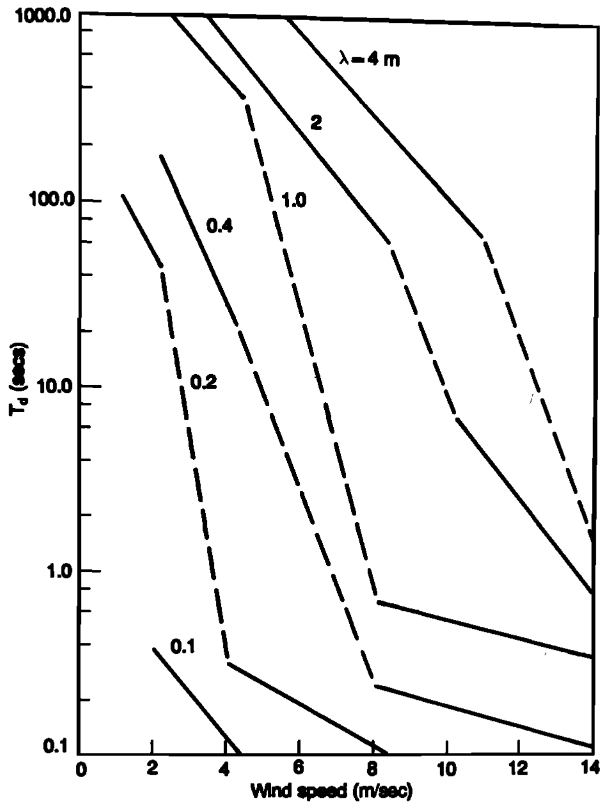

Fig. 4. The decay time (50) due to three- and four-wave interaction.

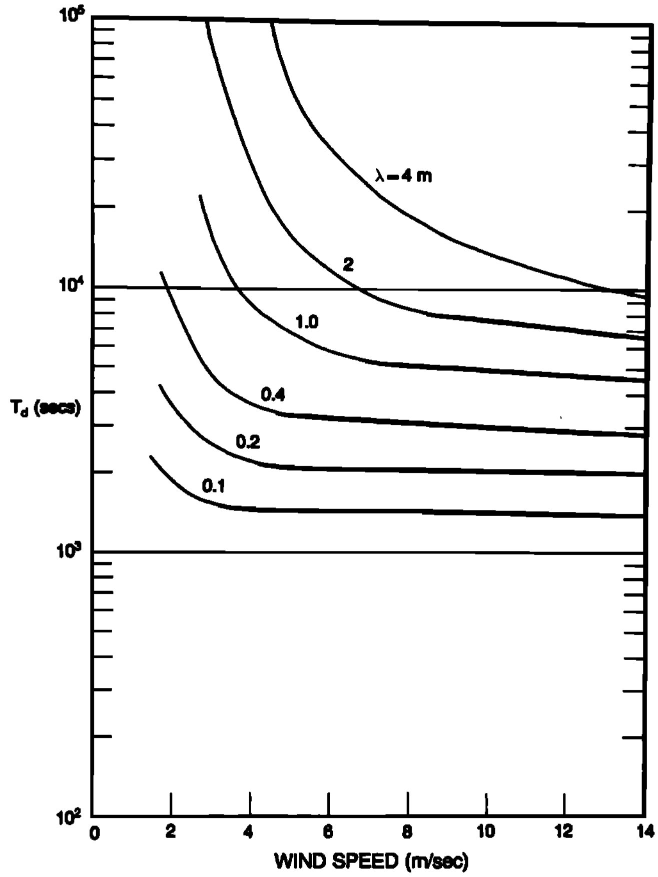

Fig. 5. The decay time (58) due to four-wave interactions.

interpolation made from T_4 (upper region) to T_3 (lower region).

A more realistic spectrum than (45) is that of *Tyler et al.* [1974]:

$$G(\theta) = \cos^S(\theta)/L(S)$$

$$L(S) = 2(\pi)^{1/2}\Gamma(\tfrac{1}{2}S + \tfrac{1}{2})/\Gamma(\tfrac{1}{2}S + 1) \qquad (51)$$

where S is a function of k.

Using (51) we evaluate (28) as

$$\sigma^2 = \eta g(k^2/l_0)[0.8\cos^2\alpha + 0.2\sin^2\alpha]$$

or

$$\sigma = 0.4(W/\lambda)(\cos^2\alpha + 0.25\sin^2\alpha)^{1/2} \qquad (52)$$

Here α is the angle of $\boldsymbol{k}$ with respect to $\boldsymbol{W}$. Use of (45), on the other hand, would replace (52) by $\sigma = 0.3(W/\lambda)$. The consequence of using the spectrum (51) does not seem very significant.

The decay time (30) obtained using the simple expression (52) is expected to be valid when

$$T_d << \frac{W}{g} \qquad (53)$$

4.4. *Decay Due to Waves of Comparable Wavelength*

For our discussion of three- and four-wave interactions we have assumed the ambient waves to have wavelengths much longer than the pattern wavelengths. This has been justified because of the peaking of the spectrum (6) at wave numbers near l_0. To further clarify this, we return to the Hasselmann equation (11). We have already considered the effects of wind and viscosity, so we now write this as

$$\frac{\partial F_p(\boldsymbol{k},t)}{\partial t} = S_{nl}' \qquad (54)$$

If we assume that F_p represents a very small perturbation on the ambient spectrum, we can write

$$S_{nl}' = -2\nu(\boldsymbol{k})F_p(\boldsymbol{k}, t) \qquad (55)$$

where

$$2\nu(\boldsymbol{k}_1) = \int d^2k_2\, d^2k_3\, d^2k_4\, G(\boldsymbol{k}_1, \boldsymbol{k}_2, \boldsymbol{k}_3, \boldsymbol{k}_4)$$

$$\cdot \left\{F_a(\boldsymbol{k}_2)[F_a(\boldsymbol{k}_3) + F_a(\boldsymbol{k}_4)] - F_a(\boldsymbol{k}_3)F_a(\boldsymbol{k}_4)\right\}$$

$$\cdot\, \delta(\boldsymbol{k}_1 + \boldsymbol{k}_2 - \boldsymbol{k}_3 - \boldsymbol{k}_4)\, \delta(\omega_{k_1} + \omega_{k_2} - \omega_{k_3} - \omega_{k_4}) \qquad (56)$$

Here G is a function of the indicated four wave numbers. A convenient simplification of this equation is given by *Dungey and Hui* [1979] for the case that F_a describes a narrow spectrum centered near $\boldsymbol{k}_1$. These authors also show that evaluation of (56) can be reduced to a single numerical integration when F_a can be represented as a sum of Gaussian functions.

To use the method of *Dungey and Hui* [1979], we have written

$$F_a(\boldsymbol{l}) = \left[\frac{\rho_0 g}{2\pi\omega_{k_1}}\right]\left[\frac{\eta}{k_1^4}\right] \exp - \left[\frac{[\boldsymbol{l} - \boldsymbol{k}_1 - (\frac{\boldsymbol{\alpha}}{2})]^2}{\beta^2 k_1^2}\right]$$

$$\cdot \exp\,[-0.74(l_0/k_1)^2] \qquad (57)$$

Here α and β are considered to be small parameters and (57) represents a "cut" out of the spectrum (4) for $\boldsymbol{l}$ near $\boldsymbol{k}_1$.

Equation (56) was evaluated for a range of values of $\boldsymbol{\alpha}$ and $\boldsymbol{\beta}$. The results are illustrated in Figure 5 for the case $\boldsymbol{\alpha} = 0, \beta = 1/3$. The quantity shown is

$$T_d = [\nu(\boldsymbol{k})]^{-1} \qquad (58)$$

We estimate that the "narrow band" approximation of Dungey and Hui is valid for $0 < \beta < 0.5$. Over this range the decay time (58) scales approximately as β^{-2}. The variation of (58) with $\boldsymbol{\alpha}$ is less than a factor of 2 for $\alpha/k_0 \leqslant 1$. We are thus led to conclude from the results given in Figure 4 and 5 that the decay rate is dominated by contributions from long ambient waves.

5. EVOLUTION OF THE PATTERN SPECTRUM

In this section we first study the evolution of the pattern spectrum (7) due to the three-wave mechanism. Using (24) we write

$$Z_p(\boldsymbol{x}, t) = B_p(0)\exp\,[i(\boldsymbol{p}\cdot\boldsymbol{x} - \omega_p t - \boldsymbol{p}\cdot\boldsymbol{R})] \qquad (59)$$

where

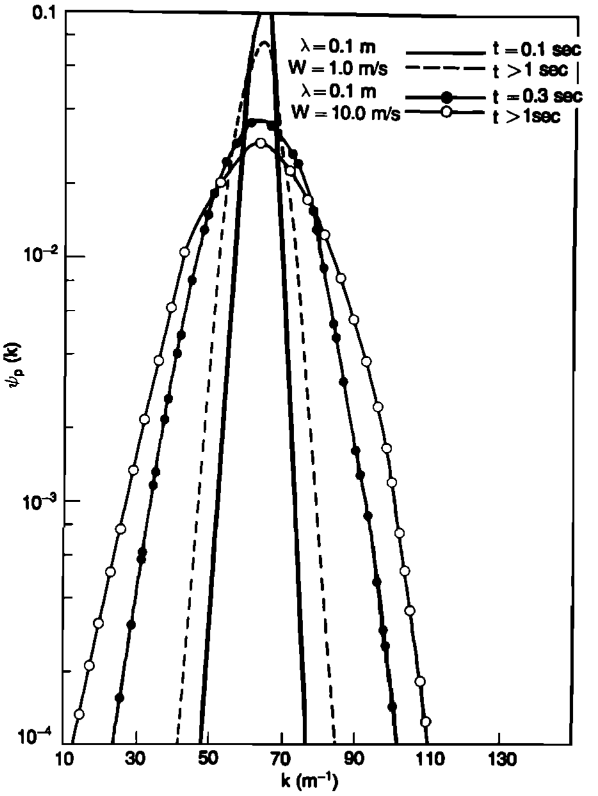

Fig. 6. The pattern spectral function (65) integrated over k_y, for the case that $\lambda = 0.1\ m$ and $p_y = 0$. Wind speeds and times are indicated.

$$p\cdot R = p\cdot\int_0^t U\,dt'$$

$$= \Sigma_l[(p\cdot\hat{l})/l]\left\{b_l e^{il\cdot x}\,[\exp(-i\omega_l t)-1] + c.c.\right\} \quad (60)$$

In (59) we have assumed the initial pattern at $t = 0$ to be a plane wave of wave number p. A more general pattern, representing a superposition of plane waves, can readily be analyzed by the present method.

The wind velocity vector $W = \hat{i}W$ is assumed to be directed parallel to the x-axis. The b_l's are supposed to be constant and to have a Gaussian distribution, with the ambient spectrum described by (4). The expression (6) can be evaluated analytically. It is consistent with the condition (23) to assume that $rl << 1$, so we obtain

$$\Gamma_p(r,t) = \tfrac{1}{2}|Bp(0)|^2 \exp(-ip\cdot r)\exp\left\{-\int d^2l\Psi_a(l)\cdot(r\cdot\hat{l})^2(p\cdot l)^2\,[l-\cos(\omega_l t)]\right\} \quad (61)$$

Equation (7) may also be evaluated analytically using the expression (61). The result gives the pattern spectrum as a function of time:

$$\Psi_P(k,t) = |B_p(0)|^2/[8\pi(c_1c_2)^{1/2}]\cdot\exp\left[-(K_x\cos\phi - K_y\sin\phi)^2/(4c_1) - (K_x\sin\phi + K_y\cos\phi)^2/(4c_2)\right] \quad (62)$$

Here

$$K = k - p$$

$$c_1 = \cos^2\phi a_1 + \sin^2\phi a_2 - 2\sin\phi\cos\phi b$$

$$c_2 = \sin^2\phi a_1 + \cos^2\phi a_2 + 2\sin\phi\cos\phi b$$

$$\tan 2\phi = 2b/(a_2 - a_1)\,, \qquad -\frac{\pi}{4} < \phi < \frac{\pi}{4}$$

$$a_1 = \int d^2l\Psi_a(l)(\hat{i}\cdot\hat{l})^2(p\cdot l)^2\,[1-\cos(\omega_l t)]$$

$$a_2 = \int d^2l\Psi_a(l)(\hat{j}\cdot\hat{l})^2(p\cdot l)^2\,[1-\cos(\omega_l t)]$$

$$b = \int d^2l\Psi_a(l)(\hat{i}\cdot\hat{l})(\hat{j}\cdot\hat{l})(p\cdot l)^2\,[1-\cos(\omega_l t)] \quad (63)$$

It is straightforward to evaluate these expressions for the spectral form (51). This is tedious and seems overly elaborate for our purpose. We therefore consider only the "peaked" spectrum corresponding to

$$G(\theta) = \delta(\theta) \quad (64)$$

and the isotropic spectrum (45).

For the peaked spectrum (64) we may simplify (62) to the form

$$\Psi_P(k,t) = \frac{|B_p(0)|^2}{4(\pi a_1)^{1/2}}\,\delta(k_y - p_y)\cdot\exp[-K_x^2/(4a_1)] \quad (65)$$

In this case

$$a_1 = p_x^2 h \quad (66)$$

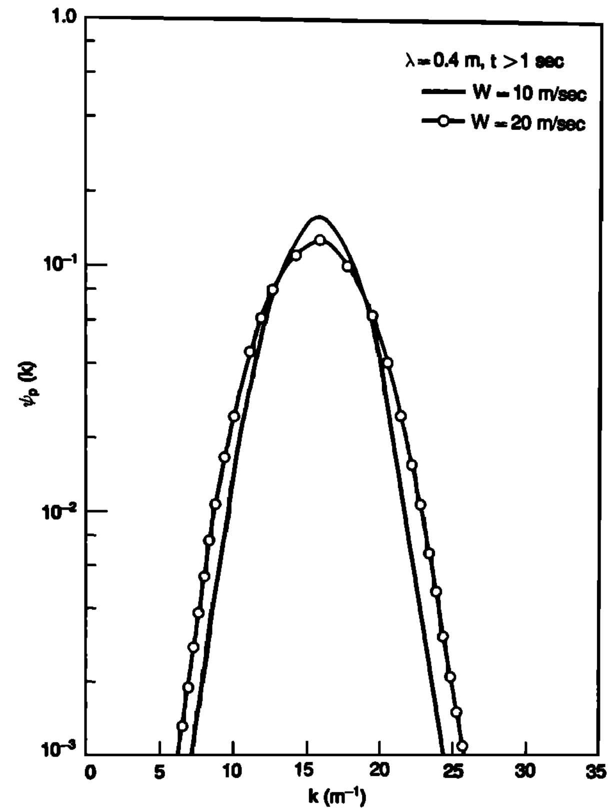

Fig. 7. The pattern spectral function for the conditions of Figure 5 for the case $\lambda = 0.4\ m$.

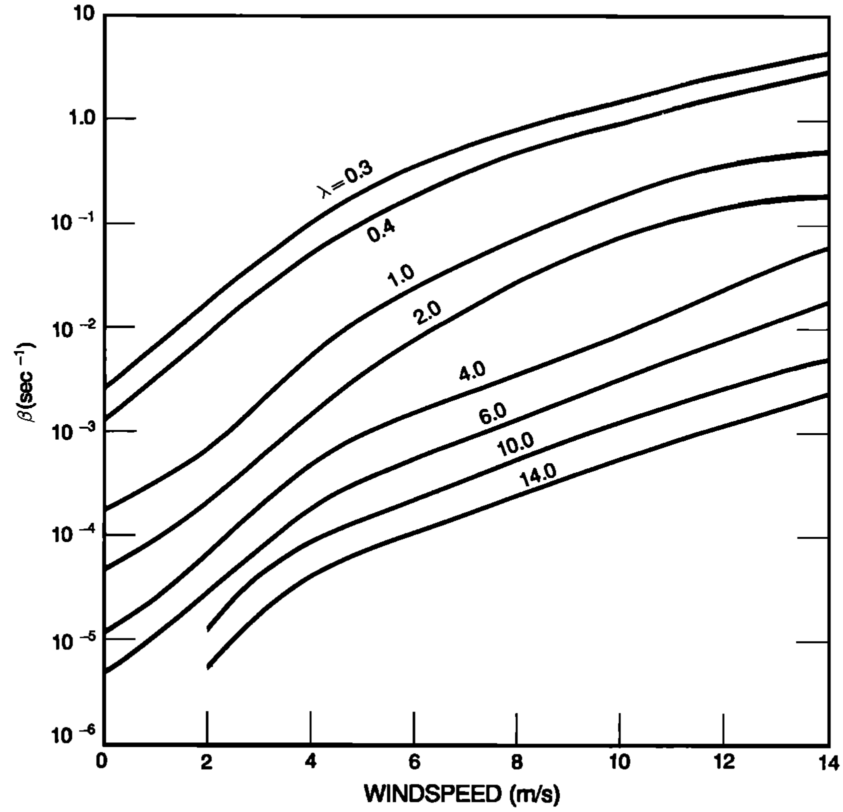

Fig. 8. The decay rate constant β of (74) as a function of wind speed for several wavelengths λ.

where

$$h = \eta \int \frac{dl}{l} \exp\left[-0.74\,(l_0/l)^2\right]\left[1 - \cos(\omega_l t)\right] \quad (67)$$

For the isotropic spectrum (25) we suffer no loss of generality in setting $p_y = 0$. Then

$$\Psi_p(k, t) = \frac{|B_p(0)|^2}{8\pi (a_1 a_2)^{1/2}} \exp\left[-(k_x - p_x)^2/(4a_1)\right] \cdot \exp\left[-k_y^2/(4a_2)\right] \quad (68)$$

Now,

$$a_1 = \frac{3}{8} p_x^2 h\,, \qquad a_2 = \frac{1}{8} p_x^2 h\,, \qquad b = 0 \quad (69)$$

where h is given by (67).

The integral (67) requires a cutoff at large l and depends logarithmically on this cutoff. Thus the scale separation condition (23) is not automatically satisfied by the spectrum (4), but must be imposed. For numerical evaluation we have done this by inserting a factor $[1 + (2l/p_x)^2]^{-1}$ into the integrand in (67). In spite of the arbitrary imposition of a scale separation, our spectral evolution equations appear to be of some interest.

As was the case with the decay, as described by (29), the spectral spreading reaches an asymptotic limit for large t. To illustrate our model, we consider the peaked model (65) for the case that $P_y = 0$. The spectrum is shown in Figure 6 for $\lambda = 2\pi/P = 0.1\ m$ and $W = 1$ and 10 m/s. In Figure 7 we show the spectrum for $\lambda = 0.4\ m$ and $W = 10$ and 20 m/s. The spectrum described by (68) is similar but evolves in both horizontal dimensions.

For these examples the asymptotic variance in the wave number is much less than the initial wave number of the wave train. Nevertheless, this spreading can decorrelate the wave phase coherence for a wave train of many wavelengths.

We have seen that four-wave interactions lead to an irreversible redistribution of wave energy in wave number space. This is described by the term S_{nl}' in (11). In the general case this is a very complex phenomena and beyond our present scope to discuss. For the case that the scale separation condition (23) can be assumed, S_{nl}' reduces to a simple diffusion mechanism

$$S_{nl}' = \frac{\partial}{\partial k_i} D_{ij} \frac{\partial F_p}{\partial k_j} \quad (70)$$

Weak interaction theory leads to the expression (see, for example, Appendix A of *McComas and Bretherton* [1977]

$$D_{ij} = \frac{1}{t} < \int_0^t k \cdot \frac{\partial U}{\partial x_i} dt' \int_0^t k \cdot \frac{\partial U}{\partial x_j} dt'' > \,, \quad t \to \infty \quad (71)$$

Here U is given by (22). For our application with the spectrum (4), the scale separation condition must be imposed by introducing a cutoff for wave numbers greater than some value, say, l_{max}. For this reason, only a brief qualitative discussion of (70) and (71) seems justified. A scalar diffusion coefficient, $D = \frac{1}{2}[D_{11} + D_{22}]$, appears sufficient, then, to characterize the diffusion. For the spectrum (51) we obtain

$$D \cong 3 \cdot 10^{-4} k^2 \omega_c\,, \qquad \omega_c = (g l_{max})^{1/2} \quad (72)$$

The variance Δk in an initial wave of wave number k is estimated at time t as

$$\Delta k = (Dt)^{1/2} = 2 \cdot 10^{-2} k (\omega_c t)^{1/2} \quad (73)$$

If we assume $\omega_c \approx 1\ s^{-1}$ as reasonable, (73) implies times of the order of 10^3 s for significant pattern distortion. This is not incompatible with the four-wave time scales of Figure 4.

6. SUMMARY AND CONCLUSIONS

We have seen that persistence times for surface gravity waves can vary from fractions of a second to many days for ocean swell [*Snodgrass et al.*, 1966]. Mechanisms studied in this paper that lead to wave pattern decay are viscous damping, air-sea interaction, and three-wave and four-wave interactions.

The three-wave interactions tend to have short time scales but do not lead to wave decay or energy transport across the surface wave spectrum. As is seen in Figures 6 and 7, these interactions lead to only a very limited spreading in wave number. If this fine spectral detail is not important for a specific application, the three-wave process should be omitted in assessing decay rates.

In this case it is convenient to summarize our calculations of surface wave relaxation in the form of single decay constant β (see *Hughes* [1978] and *Phillips* [1984] for a related model):

$$S_{nl} + S_v + S_\omega = -\beta F_p \quad (74)$$

Here we have set

$$\beta = \beta_v + \beta_w + 2\nu \quad (75)$$

(see (12), (15), and (39)), neglecting the three-wave contribution. The assumption of additivity made here appears reasonable, since for any given set of wavelengths and wind speeds, one of the three terms in (75) tends to dominate.

The relaxation rate β is shown in Figure 8 as a function of wind speed w for several wavelengths λ. At the two longest wavelengths shown the air-sea interaction gives the most significant contribution to θ. (The four-wave contribution in Figure 8 is negligible unless $\lambda << 2\pi w^2/g$).

Acknowledgments. The author would like to thank Walter Munk and Robert Hall for discussions of this paper. This work was supported partially through MITRE Corporation contract F19628-84-C-0001 and by the Office of Naval Research contract N00014-79-C-0472. This is a contribution of the Scripps Institution of Oceanography, new series.

REFERENCES

Dungey, J. C., and W. W. Hui, Nonlinear energy transfer in a narrow gravity-wave spectrum, *Proc. R. Soc. London Ser, A*, *368*, 239-265, 1979.

Garratt, J. R., Review of drag coefficients over oceans and continents, *Mon. Weather Rev.*, *105*, 915-922, 1977.

Hasselmann, K., Nonlinear interactions treated by the methods of theoretical physics, *Proc. R. Soc. London Ser.*, *A*, *299*, 77-100, 1967.

Hughes, B. A., The effect of internal waves on surface wind waves, 2, Theoretical analysis, *J. Geophys. Res.*, *83*, 455-465, 1978.

McComas, C. H., and F. P. Brethetton, Resonant interaction of oceanic internal waves, *J. Geophys. Res*, *82*, 1397-1412, 1977.

Mitsuyasu, H. and T. Honda, Wind induced growth of water waves, *J. Fluid Mech.*, *123*, 425-442, 1982.

Phillips, O. M., *The Dynamics of the Upper Ocean*, 2nd ed., Chap. 3, Cambridge University Press, New York, 1977.

Phillips, O. M., On the response of short ocean wave components at a fixed wavenumber to ocean current variations, *J. Phys. Oceanogr.*, *14*, 1425-1433, 1984.

Pierson, W. J., and L. Moskowitz, A proposed spectral form for fully developed wind seas based on the similarity theory of S. A. Kitaigorodskii, *J. Geophys. Res.*, *69*, 5181-5190, 1964.

Plant, W. J., A relationship between wind stress and wave slope, *J. Geophys. Res.*, *87*, 1961-1967, 1982.

Snodgrass, F. E., G. W. Groves, K. F. Hasselmann, G. R. Miller, W. H. Munk, and W. H. Powers, Propagation of ocean swell across the Pacific, *Philos. Trans. R. Soc. London Ser.*, *A*, *259*, 431-497, 1966.

Tyler, G. L., C. C. Teague, R. H. Stewart, A. M. Peterson, W. H. Munk, and J. W. Joy, Wave directional spectra from synthetic aperture observations of radio scatter, *Deep-Sea Res.*, *21*, 988-1016, 1974.

Van Kampen, N. G., Stochastic differential equations, *Physica*, *74*, 215-238. 1974.

Vesecky, J. F., and R. H. Stewart, The observation of ocean surface phenomena using imagery from the Seasat synthetic aperture radar: An assessment, *J. Geophys. Res.*, *87*, 3397-3413, 1982.

Watson, K. M., and B. J. West, A transport-equation description of nonlinear ocean surface wave interactions, *J. Fluid Mech.*, *70*, 815-826, 1975.

Wigner, E. P., On the quantum correction for thermodynamic equilibrium, *Phys. Rev.*, *40*, 749-759, 1932.

K. M. Watson, Marine Physical Laboratory, Scripps Institution of Oceanography, University of California, San Diego, CA 92152.

(Received February 11, 1985;
accepted August 27, 1985.)